UPGRADING GEOTHERMAL SOURCES FOR INDUSTRY: HIGH TEMPERATURE HEAT PUMP SOLUTIONS

Sven Klute[a], Matthias Lehmkuehler[a], Markus Hadam[a]

[a] Fraunhofer Institute for Environmental, Safety, and Energy Technology UMSICHT, 46047 Oberhausen, Germany, sven.klute@umsicht.fraunhofer.de CA

Abstract:
Geothermal energy is a continuously available and reliable heat source, making it inherently well suited for industrial process heat supply. However, its application is often limited by an insufficient temperature level of the geothermal source. High temperature heat pumps (HTHPs) can overcome this barrier by extracting heat from geothermal brine and delivering it at higher temperatures to the industrial process. This paper focuses on the selection of suitable heat-pump cycles for different industrial heat carriers and the necessary adaptation to be made for an operation with a geothermal source. The paper presents a thermodynamic comparison of different HTHP cycles for an exemplary geothermal source (85 °C) paired with process water, steam and air at a temperature level of 120 °C. The simulation results are compared with reference implementations at industrial sites and manufacturer data to assess technical feasibility. The results show that a wide range of industrial applications can already be accessed with state-of-the-art components and that appropriately selected HTHP cycles can significantly increase the COP (up to 29–43 %) and the applicability of geothermal resources in industry.

Keywords:
geothermal energy, high-temperature heat pumps, process heat, renewable energy

1. Introduction

Process heat is one of the most important energy demands in the industrial sector. In Germany, for example, about 67 % of industrial energy consumption is used to provide process heat [1]. Due to technical and economic constraints, less than 6 % of this heat is currently supplied by renewable energy sources [2]. Geothermal energy has great potential to increase this share since it is reliable and a continuous source of heat. To date, the industrial use of geothermal energy remains limited (see *Table 1*). Currently, only 0.7 % of the installed geothermal capacity (equivalent to 852 MW) is used for industrial purposes across 14 countries [3].

Table 1. *Installed capacity of geothermal power generation and direct utilization in 2020 [3], [4]*

Utilization	Capacity [MW]	Share [%]
Total	123,677	100
Power Generation	15,950	12.9
Direct utilization (sum)	107,727	87.1
Geothermal heat pumps (ground-source)	77,547	62.7
Space heating	12,768	10.3
Bathing and swimming	12,253	9.9
Greenhouse heating	2,459	2.0
Aquacultural pond heating	950	0.8
Industrial use	852	0.7
Other	798	0.7

However, a positive trend can be observed in industrial applications (see Figure 1). Over the past 20 years, installed capacity has increased exponentially, as industries worldwide strive to become more sustainable and less dependent on imported energy sources. Compared to the overall growth of geothermal energy, this increase is modest and accounts just for a small portion of the total installed capacity.

Industrial applications tend to be large facilities with high energy demands and often operate nearly year-round, resulting in the highest capacity utilization rate among geothermal applications (0.61 on average) [5].

Process heat is, however, a lot more versatile compared to other geothermal applications like district heating or power generation. Not only the process itself might vary (e. g. cooking, distillation, drying, washing and sterilization), but also the process media (e. g. hot water, steam, air, thermal oil), resulting in increased design complexity. In addition, the temperature requirements are generally much higher than other applications like district heating or bathing, making integration technically challenging. In the past, thermal upgrading was avoided due to increased cost and technical limitations. Instead, suitable heat consumers that could be supplied directly from the geothermal source were targeted [6].

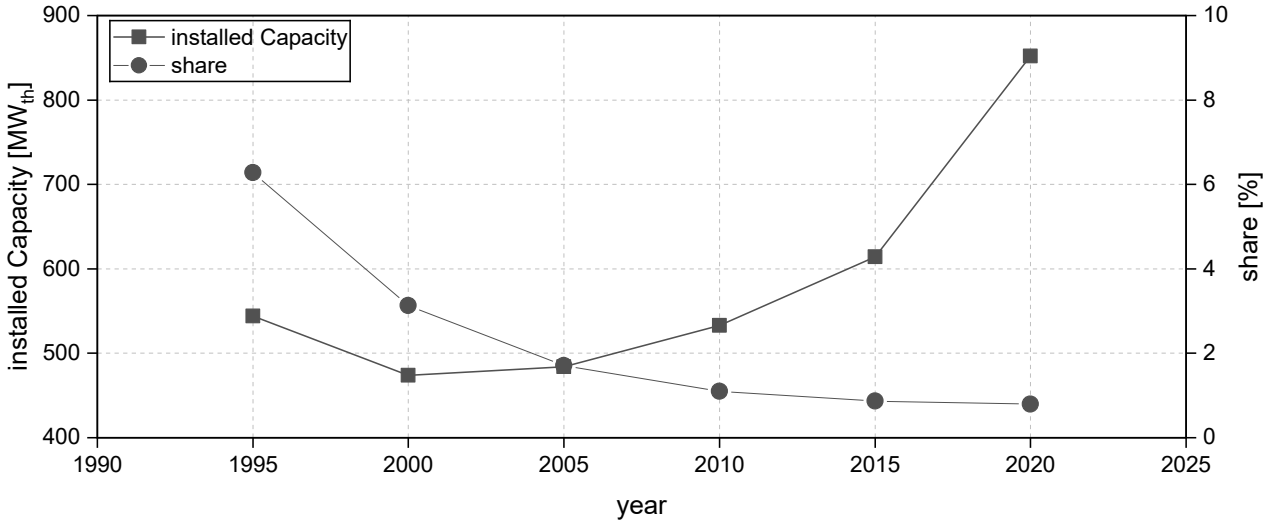

Figure 1. *Development of the installed capacity for industrial use of geothermal energy and the share of total installed capacity from 1995 till 2020. Based on data from [3], [4]*

In recent years, the technology readiness level (TRL) of high temperature heat pumps (HTHP) has improved significantly. According to the findings of IEA Annex 58, large scale heat pumps (> 10 MW_{th}) with supply temperatures exceeding 120 °C are expected to be commercially available and established by 2027–2029. For medium sized systems (up to 10 MW_{th}) temperatures of more than 160 °C are expected by 2027–2029 [7]. This development offers great potential for industrial use of geothermal energy, as the lack of suitable HTHPs has historically been a limiting factor in industrial use of geothermal systems. The modifications required for the integration of a heat pump (HP) are relatively minor and are presented in Chapter 2 using operational examples from demonstration plants for hot water, steam, and hot air supply. In addition to these existing examples, a case study is conducted to demonstrate the future potential for industrial process heat supply via geothermal energy (Chapter 3 and 4).

2. Industrial use of geothermal energy through heat pumps

The design of a geothermal plant for industrial purposes is strongly influenced by the thermodynamic properties of the geothermal source. Most current applications use high-enthalpy hydrothermal systems in which dry steam or a two-phase mixture is extracted and processed. In these systems, an additional HP is typically not required, as the temperature level of the source is already sufficient. For low-enthalpy systems on the other hand, HP integration is often necessary, as liquid water is extracted on a moderate temperature level. A simplified layout of such a system is shown in Figure 2. In most systems, a closed-loop geothermal water system is used to prevent the transfer of unwanted components of the geothermal water such as dissolved gases [8]. Electrical submersible pumps or line shaft pumps are installed in the production well to extract the geothermal water [9]. In order to compensate for pressure fluctuations in the system, pressure equalization tanks filled with a mixture of geothermal water and inert gases are used [10]. The operating pressure of the system is usually up to 16 bar or higher [11]. After coarse filtration (e. g. by backwash, basket and bag filters [10]), heat is extracted via shell-and-tube, bolted or welded plate heat exchangers [10], [11]. For most applications, an intermediate loop is implemented. This prevents contamination of the process fluid by geothermal water and vice versa. The intermediate loop also prevents potential corrosion or scaling problems caused by the mineral content of the geothermal fluid in the process equipment or heat exchangers of the HP. Multiple heat exchangers can be used in parallel to ensure continuous operation during maintenance work (e. g. cleaning of the heat exchangers). The heat exchanger material is selected based on the geothermal water composition. For highly corrosive fluids, titanium is used instead of stainless steel [11]. If the system pressure is not sufficient to overcome the pressure losses in the injection borehole, additional injection pumps must be installed. As these pumps can be installed above ground, no special pump designs are required [9]. As a result of cooling the temperature of the geothermal fluid, precipitation, scaling and changes in chemical

properties (e. g. pH value) of the geothermal water can occur. To prevent damage to the injection borehole, fine filters are therefore installed prior to injection [11].

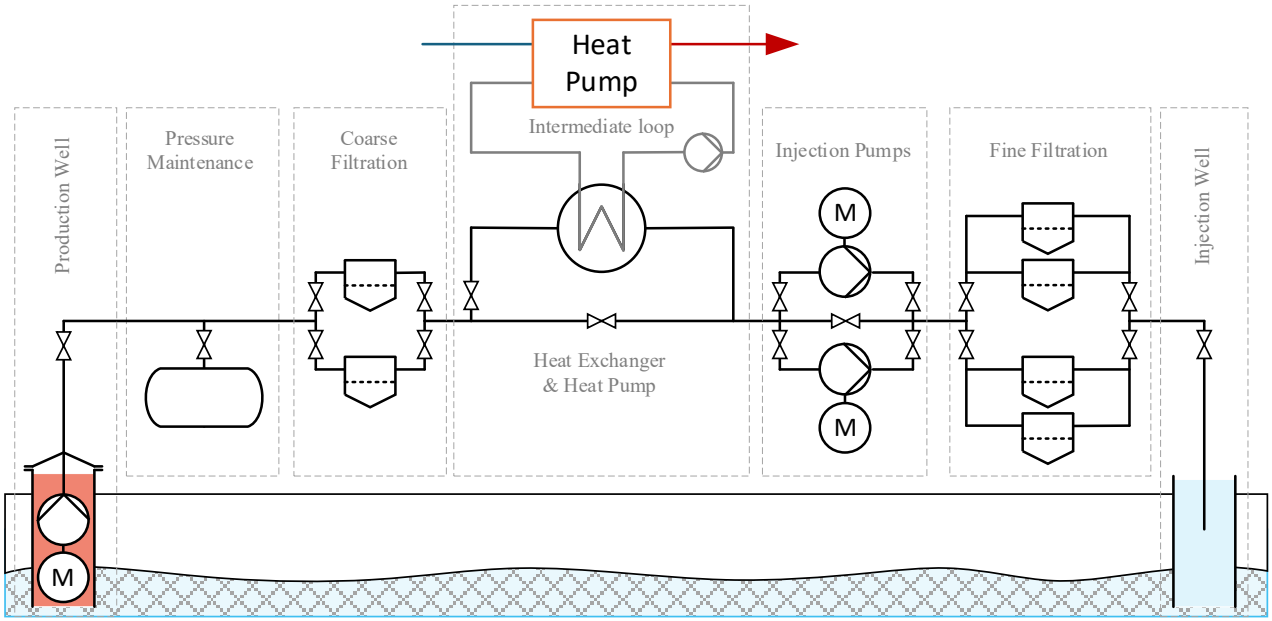

Figure 2. *Typical layout of a geothermal plant for heat generation with heat pumps adapted from [11]*

Installing a HP generally requires only minor modifications, as it can be integrated at the conventional heat extraction point of other applications like district heating. If large temperature glides of the geothermal source are desired, several HPs can be arranged in series to improve the overall efficiency. At some locations, however, the injection temperature must stay above a certain value (e. g. 50 °C) to prevent negative effects on the reservoir and the subsurface [12].

The HP-cycle is not further restricted by the geothermal source and can be adapted according to the specific use-case. When designing the HP, particular attention must be paid to the process heat transfer medium, as it has a decisive influence on the specific design of the HP-cycle. Typically, hot water (Section 2.1), steam (Section 2.2), air (Section 2.3) are used. Examples of operating and recently commissioned installations are presented in the following sections. Since industrial examples are relatively sparse, representative examples of comparable heat sinks are presented whenever no industrial example could be found.

2.1. Process water

Process water is used for several industrial applications such as washing, cleaning and process heating. Above 100 °C, pressurized systems are used to prevent the water from boiling. The use of HPs with geothermal energy as a heat source has been investigated in several preliminary studies. However, no operating example has been found. Beardsmore et al. [13] present a concept of a planned geothermal district heating network, which is considered to be connected to a new industrial park. A dairy processing facility and a bottling plant were identified as possible consumers. In both cases, geothermal energy from a 68 °C aquifer is fed into the district heating network and transferred to the end-user. The HP of the bottling plant is designed to reheat process water from 92 °C to 98 °C with district heating water as a source (53 °C/ 38 °C) and has a thermal peak load of 1.2 MW. The coefficient of performance (COP) is estimated to be around 3.7. The HP of the dairy processing plant is operated with district heating water (53 °C/37 °C) as a source and process water as a sink (80 °C/ 71 °C). The COP of this setup is around 4.7 with a thermal peak load of 1.7 MW.

Apart from industrial utilization, operating examples can be found especially in geothermal district heating networks (GDHN). In Schwerin (GER) 4 HP units (7,350 MW_{th}, R134a) were installed in 2024. Geothermal energy from a depth of 1,340 m at 56 °C and a flow rate of 41.6 kg/s is used as a source to provide heat for the GDHN at about 80 °C. [14]

In Aarhus (DK), a GDHN is currently under construction and planned to be extended by 12 HPs units (9.6 MW_{th}) [15]. In the presented simplified concept, geothermal fluid with 75 °C is first used to preheat the DH return flow from 41 °C to 73 °C and then used to heat a secondary loop which is used by the HP as a heat source (41 °C/ 8 °C). On the sink side of the HP, preheated district heating water is further heated (90 °C/ 73 °C). Similar operating conditions are found in Neuruppin (GER), where 5 cascaded HPs are currently under construction to provide 3.3 MW_{th} for a district heating network. Geothermal water with 70 °C is used to supply heat at 90 °C [16]. Other examples are found in Erding (1 MW_{th}, in operation since 2020), Poing (2.5 MW_{th}, in operation since 2023) and Straubing (1.2 MW_{th}, source 36 °C, sink 72 °C, in operation since 2016) [17].

In addition to these recent developments, thermally driven absorption HPs have been in operation in Denmark for decades. In Thisted, a GDHN that was initially equipped with an electrically driven HP (1984) was gradually extended by an absorption HP (4 MW_{th}) in 1988 and a second unit of 7 MW_{th} heating capacity in 2001. Geothermal water is cooled from 43 °C to 11 °C in order to reheat the DH water (42 °C/ 72 °C). As driving input, heat from a straw-boiler and incineration CHP plant is used (150 °C/ 130 °C). At another site in Copenhagen, a series configuration of two-stage absorption HPs supplies 27 MW_{th} to the district heating network (50 °C/ 85 °C) from geothermal energy (74 °C/ 17 °C) since 2005. A similar setup with 4 serial connected two-stage absorption HPs was installed in Sonderborg in 2013. The system is designed to supply 12 MW_{th} to a district heating network (44 °C/ 82 °C) from geothermal energy (48 °C/ 15 °C). The driving heat is supplied by two wood chip boilers. [18]

The examples for process water demonstrate that HP integration with geothermal sources is well established for hot water supply, particularly in district heating. The system configuration is directly transferable to industrial applications, where the primary difference lies in higher required supply temperatures, which can be addressed through appropriate HTHP cycle and refrigerant selection.

2.2. Process steam

The generation of process steam from geothermal sources has been investigated in detail in [19] and [20]. In theory, numerous approaches on how to integrate HPs pumps into steam networks have been discussed, but only a limited number has been tested in prototypes or demonstrators to date.

The R&D project STEPs developed and tested a demonstrator with a two-stage compression HP. The system was designed to operate with geothermal energy but was tested with freshwater (52–97 °C) instead. The target temperature of the steam was in the range of 120–150 °C. On a laboratory scale (150 kW_{th}) process steam at 150 °C was successfully generated from a source temperature of 65 °C with a COP of 2.1 [21].

In the UK, a distillery is developing a demonstrator to utilize waste heat from a geothermal power plant to generate steam [22]. Hot water at 80 °C is used as a heat source for the steam-generating HP, which supplies steam at around 120 °C for the distillery. The return water of the process (60–70 °C) is further used for miscellaneous on-site heat demands. In the first phase of the project, different HP technologies were compared. The standard HP cycle achieved an estimated COP of 4. MVR systems can raise the COP to 5.95 but increase the initial investment by a factor of 4–5. The demonstrator is designed at 25 % of the intended full-scale capacity. Additional examples of steam generating HPs in operation can be found in the IEA Annex 58 and Annex 68 databases [23].

The examples above show that process steam generation via HP has been successfully demonstrated at prototype and pilot scale, though mostly independent of geothermal sources. Since the integration on the source side remains unchanged, these configurations are directly transferable to geothermal systems. The main challenge lies in achieving sufficiently high supply temperatures for process steam, which can be addressed through appropriate HTHP cycle selection, particularly in combination with MVR.

2.3. Hot air

The supply of hot air from geothermal energy has been mostly used in the context of agricultural drying. The majority of these applications are designed to work without a HP (e. g. [24], [25] or [26]) at moderate sink temperatures (e. g. 45–80 °C). Two HP demonstrators can be found in Thailand. The first demonstrator is designed as a single-stage system and achieves a COP of 3 with geothermal water at around 50 °C and air outlet temperatures of about 73 °C. The two-stage system was tested with geothermal water at 45 °C and an air outlet temperature of 84 °C with a COP of about 4.2. In both cases, hot air is supplied indirectly via an intermediate water cycle [27]. No example of a geothermal HP with direct air heating was found.

Apart from geothermal applications, few examples can be found in industrial settings. The demonstrator of the R&D project DryFiciency was installed at the brick drying facility in Uttendorf (Austria). The closed loop HP (400 kW_{th}) uses waste heat as a heat source to provide 160 °C of hot air. An intermediate water cycle is used to transfer the heat to the process fluid (air) [28].

Existing examples demonstrate that hot air supply via HP is technically feasible, although applications remain limited to low temperatures or non-geothermal heat sources. The use of intermediate water loops, as seen in current demonstrators, aligns well with the typical layout of geothermal systems and allows for a straightforward integration. To reach the higher temperature levels required by industrial hot air processes, the selection of suitable HTHP cycles and refrigerants becomes essential.

3. Description of the case study

As presented in Chapter 2, HTHPs are increasingly being implemented in geothermal systems as well. To demonstrate this potential further, a case study is presented in this paper. A geothermal source with a moderate temperature level of 85 °C is used to provide process heat at a common temperature level of 120 °C. The importance of proper cycle and refrigerant selection is demonstrated for three different sink fluids (hot air, process water and process steam) with varying temperature glides (difference between inlet and outlet temperature). Four common HP cycles (six for steam generation) and 12 different refrigerants are compared for each combination of sink and source.

3.1. Heat pump cycles

The HP-cycles are implemented in Dymola (v. 2026x) with the object-oriented programming language Modelica (v. 4.1). The models of the HP components are based on the open-source library ClaRa (v. 1.8.0) and are adapted to meet the requirements of this study. More detailed information on the models can be found in [19]. The six investigated HP-cycles are presented in Figure 3. The geothermal source and the evaporator of the HP are separated by an intermediate water loop which is not shown in the figure. The electricity demand of the circulation pump is relatively small and therefore neglected. Since this case study focuses on the effect of different combinations of HP-cycles and refrigerants, the production and injection pump of the geothermal source are neglected as well. All heat exchangers are modelled as ideal counterflow heat exchangers without pressure losses and a pinch temperature of 5 K. The compressors have an isentropic efficiency of 0.75 and an electrical efficiency of 0.98. The throttle is assumed to be isenthalpic.

In Figure 3, cycles A and D represent the standard vapor compression cycle and include an evaporator, a compressor, a condenser and a throttle. Cycle A is designed to operate at subcritical conditions, while cycle D is operated as a trans-critical cycle. The upper pressure level of the trans-critical cycle is simplistically assumed to be 10 bar above the critical pressure and is therefore not optimized for the individual operation conditions. The cycle B is equipped with an additional internal heat exchanger (IHX), which was individually adjusted for each refrigerant and boundary condition. Cycle C represents a cascaded HP with separate bottom and top cycles and a shared intermediate condenser/evaporator. Cycles E and F are solely used for steam generation and introduce an additional MVR to the standard subcritical cycle (A) and the IHX cycle (B). In both cycles, the closed-loop HP supplies saturated steam at 1.1 bar. After MVR compression, water is injected to cool the superheated steam to saturated conditions.

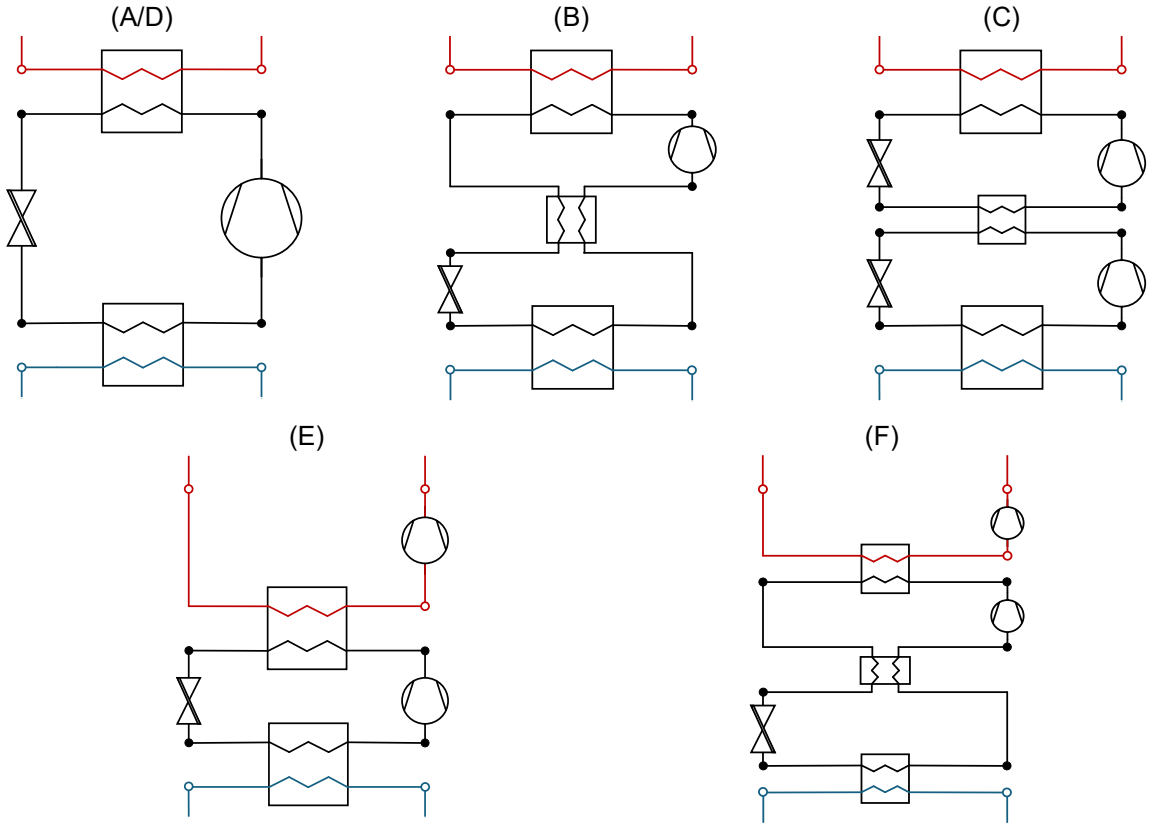

Figure 3. *A: Standard cycle (subcritical), B: IHX-Cycle (internal heat-exchanger), C: Cascade cycle, D: Standard cycle (trans-critical), E: Standard cycle (subcritical) + mechanical vapor recompression, F: IHX-Cycle + mechanical vapor recompression*

3.2. Boundary conditions for sink and source

For the geothermal source, a moderate temperature of 85 °C and a production rate of 100 kg/s are used for all three sinks. The temperature level was deliberately chosen to be moderate to reflect the more challenging operating conditions associated with lower source temperatures. Many geothermal sources provide significantly higher temperatures, which increases the suitability for industrial applications. The temperature profiles of the sinks (hot air, process water and process steam) are qualitatively illustrated in Figure 4. All three sinks share a target temperature of 120 °C and a heating capacity of 10 MW_{th}. The water (60 °C) and air (15 °C) sinks have a sensible temperature profile and require large temperature glides of 60 K and 105 K, respectively. For the supply of process steam, hot water at 100 °C needs to be preheated first, before it is fully evaporated to saturated conditions (120 °C, ~1.99 bar). The temperature glide of the steam sink is 20 K. The boundary conditions described result in crossing and non-crossing temperature profiles, which need to be considered when evaluating the HP performance (see Section 3.4).

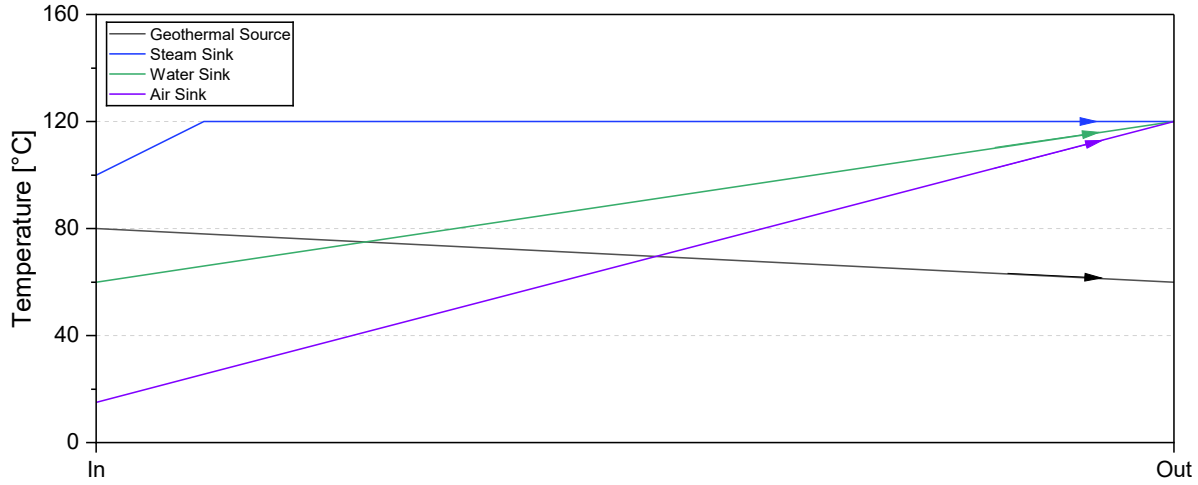

Figure 4. *Qualitative overview of temperature profiles for the source and sinks (water, steam, air)*

3.3. Refrigerants

A total of 12 refrigerants were selected for this case study (Table 2*)*. The refrigerants were selected based on their ozone depletion potential (ODP), global warming potential (GWP) as well as their critical conditions and the availability in the refrigerant library of the simulation environment. R1234yf, R1234ze(E), R290 and E170 are solely used in the bottom cycle of the cascaded HP. For the trans-critical cycle, R1234ze(Z), R1233zd(E) and R600 are chosen. The open MVR cycle for steam generation is operated with R718.

Table 2. *Properties of the investigated refrigerants. HCFO = Hydrochlorofluoroolefins; HFO = Hydrofluoroolefins; HC = Hydrocarbons; T_c = critical temperature; p_c = critical pressure; ODP = ozone depletion potential; GWP = global warming potential; SG = safety group [29]*

No.	Type	Name	T_c [°C]	p_c [bar]	ODP	GWP	SG
1	HCFO	R1233zd(E)	166.5	36.2	0.00034	1	A1
2	HFO	R1234ze(Z)	150.1	35.3	0	<1	A2L
3	HFO	R1234yf	94.7	33.8	0	<1	A2L
4	HFO	R1336mzz(Z)	171.3	29.0	0	2	A1
5	HFO	R1234ze(E)	109.4	36.3	0	<1	A2L
6	HC	R600a	134.7	36.3	0	3	A3
7	HC	R601a	196.6	33.7	0	0	A3
8	HC	R290	96.7	42.5	0	3	A3
9	HC	R600	152.0	38.0	0	4	A3
10	Natural	R718	373.9	220.6	0	0	A1
11	Natural	R717	132.3	113.3	0	0	B2L
12	Ether	E170	127.2	53.4	0	1	A3

3.4. Evaluation criteria

The comparison of the HP cycles is based on thermodynamic performance criteria. Since both the heat sink and source have a large temperature glide (difference between inlet and outlet temperature), Lorenz efficiency is used as a reference instead of Carnot efficiency. In the following, just the fundamental equations for better understanding are presented. Further details about the individual equations can be found in [7].

The COP is calculated using the simulation model and is defined as the ratio of the heat provided at the desired temperature level and the required electrical energy input (Eq. (1)). The Lorenz efficiency compares the COP to a reference process to evaluate how close it is to a thermodynamic reference process (Eq. (2)). In this paper, Lorenz cycle is chosen as reference process, which can be estimated according to Eq. (2–4).

$$COP = \dot{Q}_{use} \ / \ P_{el} \tag{1}$$

$$COP_L = \bar{T}_{sink} \ / \ (\bar{T}_{sink} - \bar{T}_{source}) \tag{2}$$

$$\bar{T}_{sink} = \ \Delta T_{sink} / \ ln(T_{sink,out} / \ T_{sink,in}) \tag{3}$$

$$\bar{T}_{source} = \ \Delta T_{source} / \ ln(T_{source,in} / \ T_{source,out}) \tag{4}$$

$$\eta_L = \ COP / \ COP_L \tag{5}$$

Whenever the HP is operated with crossing temperature profiles, a certain amount of supplied heat can be transferred by direct heat exchange instead. For a better comparison, COP must be separated into a direct heat exchange and a HP part following Eq. (6–9). Note that the $COP_{L,HP}$ is different from the COP_L and needs to be recalculated for the relevant temperature segment of the HP part. The mean temperature lift of the HP can be calculated according to Eq. (10). In the following, the HP part is used for the analysis.

$$x_{direct} = (T_{source,in} - \ T_{sink,in}) \ / \ (T_{sink,out} - \ T_{sink,in}) \tag{6}$$

$$x_{HP} = (T_{sink,out} - \ T_{source,in}) \ / \ (T_{sink,out} - \ T_{sink,in}) \tag{7}$$

$$COP_{HP} = \ COP * \ x_{HP} \tag{8}$$

$$\eta_{L,HP} = \ COP_{HP} / \ COP_{L,HP} \tag{9}$$

$$\Delta\bar{T}_{lift,HP} = \ \Delta T_{sink} / \ ln(T_{sink,out} / \ T_{sink,in}) - \Delta T_{source} / \ ln(T_{source,in} / \ T_{source,out}) \tag{10}$$

4. Results and discussion

The results of the simulations will first be discussed individually for each sink and will then be compared collectively. In the individual sections, two graphs are presented. The graph on the left-hand side plots all evaluated data points with their corresponding COP and mean temperature lift for the HP part. For sinks with crossing temperature profiles (process water and air), the best and worst combinations of each cycle and refrigerant are re-calculated with hypothetical on-site preheating (to 80 °C) to indicate the potential for improvement (grey data points).

4.1. Steam

For steam generation, a COP in the range of 2.49–3.68 is estimated (Figure 5). The highest COP (3.68) is achieved with the IHX cycle (R601a) and MVR (cycle F). The additional MVR component increases the COP of the standalone IHX by roughly 7.3 %. Cycle A, B, and C achieve COP values well above 3 when R1233zd(E) is used as a refrigerant. Furthermore, all three cycles show a large COP spread (delta COP: A~0.74, B~0.61, C~0.74), which underlines the importance of proper selection of refrigerants. The lowest COP (2.49) is achieved when using cycle A and R600a. The trans-critical cycle shows poor performance with all three tested refrigerants and proves to be unfavourable when supplying steam.

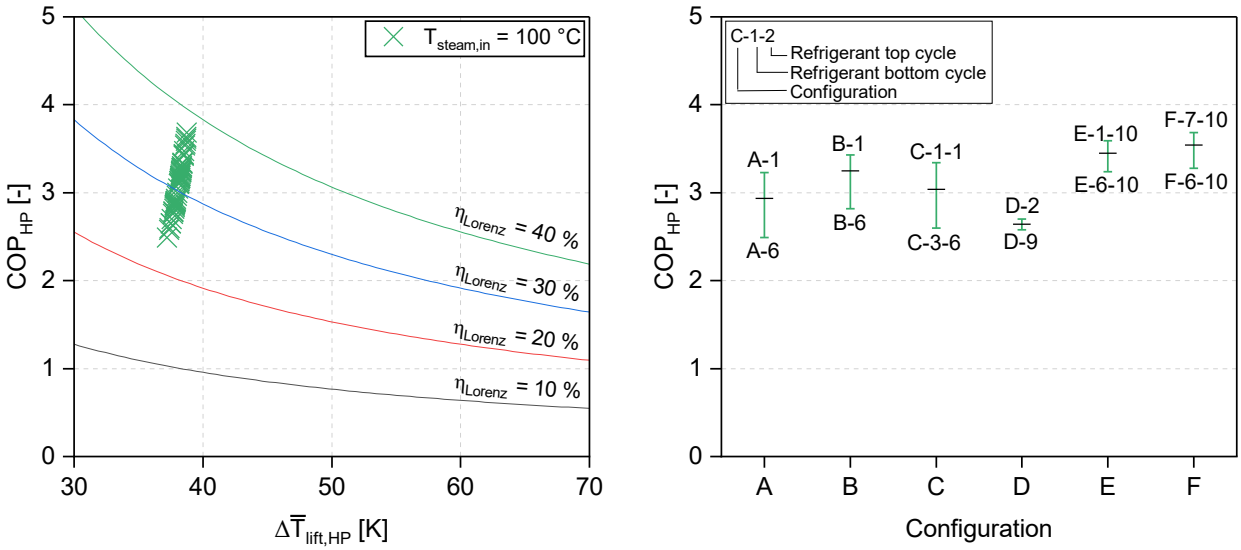

Figure 5. *COP of the calculated configurations (left) and COP range for each HP cycle for the steam sink*

4.2. Water

The COP for the water sink is in the range of 1.94–2.75 (Figure 6). The sensible heat profile with a larger temperature glide generally leads to lower COPs compared to the steam sink. Overall, the trans-critical cycle shows the best performance, especially when R600 is used. Cycles A, B, and C (top cycle) reach their maximum when using R1234ze(Z). The lowest COP value is reached by the cascade system with R1234yf in the bottom cycle and R600 in the top cycle. Cycle A and B are less influenced by the choice of refrigerant when compared with the steam sink. For cycle C, however, a similar effect can be observed (delta COP: ~ 0.7).

Preheating the water (e. g. by waste heat) from 60 °C to 80 °C has a positive effect on the COP of all investigated configurations and emphasizes the importance of proper HP integration. A direct comparison of the COP is, however, not sufficient, since the HP is designed to deliver 10 MW_{th} while additional energy is added to the system by preheating. The results provide an indication on how the overall system might be improved and should not be used for a direct comparison. Preheating leads to a reduction of the temperature glide on the sink side and favours the use of subcritical cycles instead of the trans-critical cycles. The highest COP values are achieved with R1234ze(Z) and cycles B (3.72), C (3.52), and A (3.51) respectively. For the trans-critical cycle, the COP increases to 2.96.

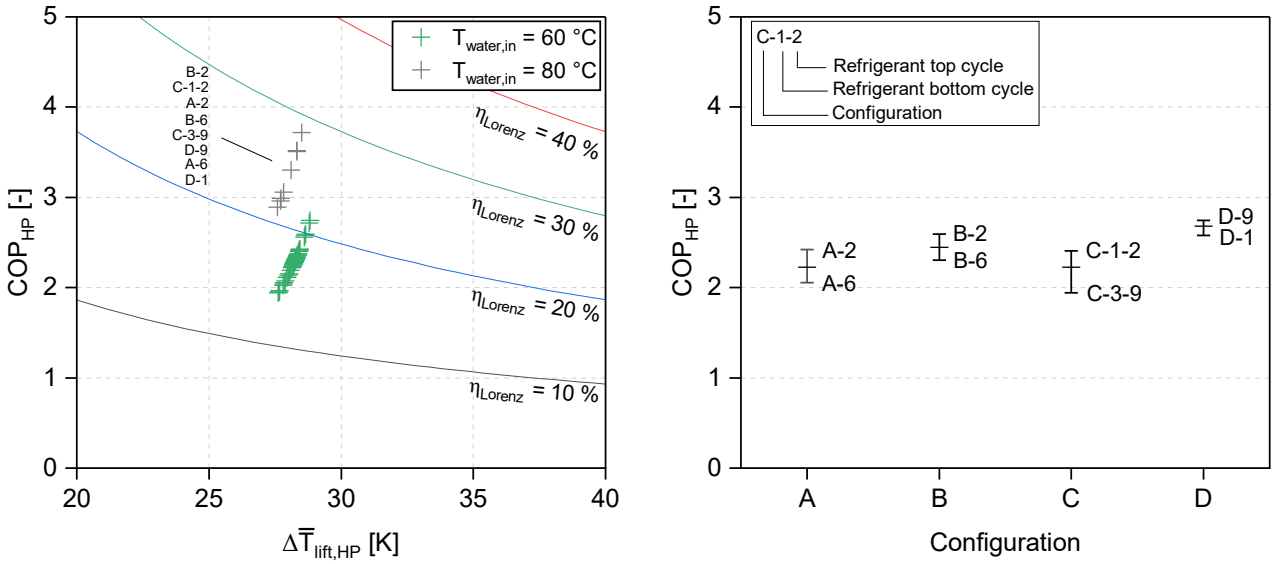

Figure 6. *COP of the calculated configurations (left) and COP range for each HP cycle for the water sink*

4.3. Hot Air

The air sink was designed to have a high temperature glide of 105 K, leading to generally lower COP values in the range of 1.11–1.97 (Figure 7). The overall ranking of the cycles is similar to the water case with minor changes in the choice of the refrigerant. For the lowest COP of cycle A, refrigerant 9 is used instead of refrigerant 6, and for the lowest COP of cycle B refrigerant 7 instead of refrigerant 6. The highest COP values

are achieved by the trans-critical cycle with R600 (1.97) and the IHX cycle with R1234ze(Z) (1.90). R1234ze(Z) shows the best performance for cycles A, B, and C when used in top cycle. The lowest COP is achieved by the cascaded system with R1234yf in the bottom cycle and R600 in the top cycle.

Preheating the air (e. g. by waste heat) from 15 °C to 80 °C increases the COP range to 3.06–3.72. Similar to the water case, a direct comparison of the COP data should be avoided. The reduced temperature glide on the sink side favours the use of subcritical cycles. The IHX cycle (B) achieves the highest COP (3.72) when using R1234ze(Z). Cycles A and C reach slightly lower values (3.51 and 3.52) with the same refrigerant. For the trans-critical cycle, R1234ze(Z) achieves the highest COP of 3.61.

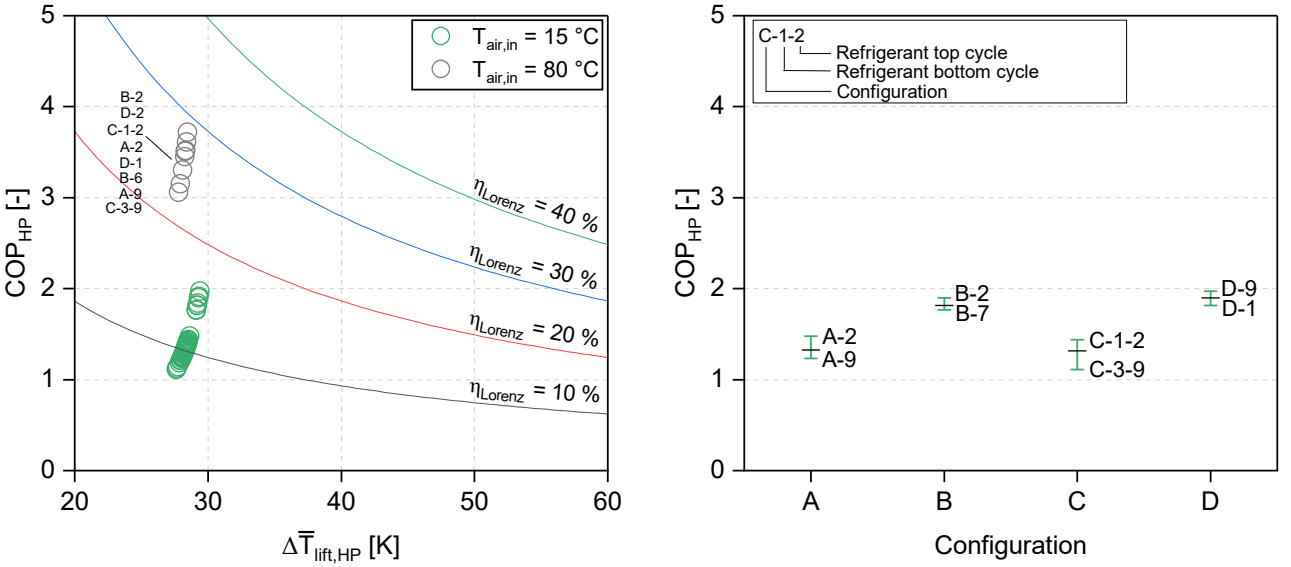

Figure 7. *COP of the calculated configurations (left) and COP range for each HP cycle for the air sink*

4.4. Comparison with HTHP data

The calculated results are plotted alongside reference data from HP suppliers compiled within IEA Annex 68 in Figure 8. The orange datapoints represent applications with non-crossing temperature profiles and are generally higher than those of applications with crossing temperature profiles (blue). The results for the steam sink of this case study show a good fit with the reference data and achieve COP values in the lower to mid-range (η_L ~0.25–0.39). The water and air sinks, on the other hand, are calculated with a large temperature glide on the sink side and reach COP values at the lower end of the reference data. Preheating significantly increases the COP of both sinks but does not change the overall ranking when compared with the reference data (orange).

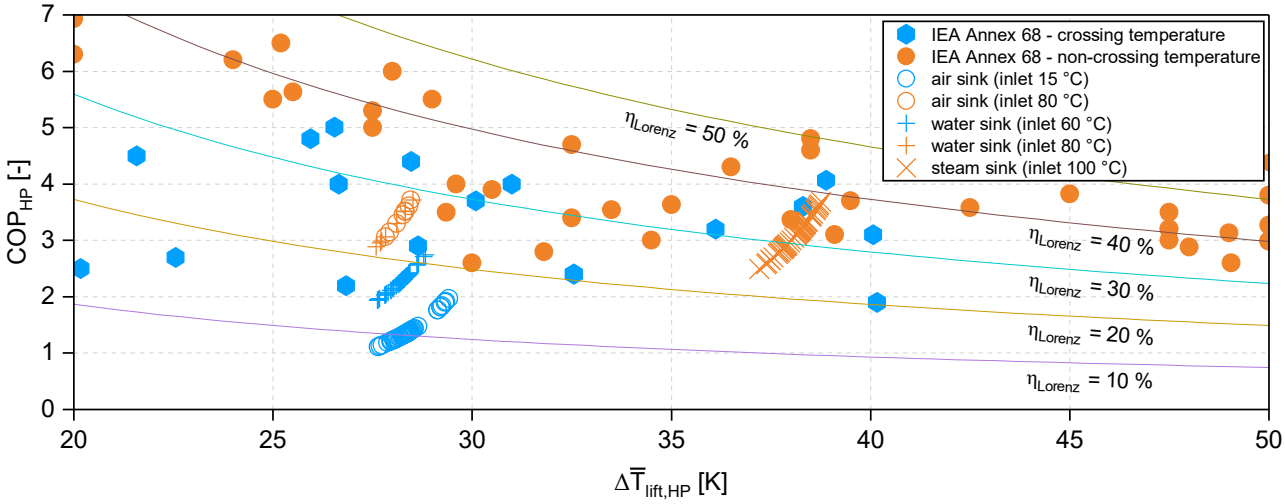

Figure 8. *Comparison of calculated data with reference datapoints from IEA Annex 68 [23]*

The results of this case study are within a plausible range but highlight room for improvement. It should be noted that the simulations were conducted with conservative assumptions (e. g. isentropic compressor efficiency of 0.75, pinch point temperature difference of 5 K could be reduced to ~3 K) and without cycle-

specific optimization. The geothermal source does not impose any additional thermodynamic penalty compared to other water-based heat sources, confirming its suitability for HTHP integration. Even under these conservative assumptions, the achieved COP ranges indicate a significant advantage over direct electric heating (COP = 1) and are competitive with conventional boiler systems when considering primary energy factors. The constant and predictable temperature level of the geothermal source is particularly advantageous for HTHP operation, as it enables stable, year-round performance without the seasonal or process-dependent fluctuations typically associated with waste heat or ambient air sources. Moreover, as a renewable and therefore virtually inexhaustible heat source, geothermal energy enables a significant reduction in fossil fuel dependency and associated CO_2 emissions, further strengthening the case for its integration with HTHPs in industrial settings.

5. Conclusion

Geothermal energy is as a suitable heat source for industrial process heat. The technical adaptations for HP integration are relatively minor. Most systems use an intermediate loop to prevent contamination of the heat carrier or product in case of leakages and to reduce technical problems such as corrosion inside of the HP or process equipment. The availability of HPs with supply temperatures above 100 °C used to be a limitation but has been overcome in recent years. Steam and hot water supply with (geothermal) HPs have been proven in industrial settings. For hot air supply, first implementations are planned and tested in demonstrators.

The HP cycle and refrigerant need to be carefully matched to the specific boundary conditions (e. g. temperature levels, glide and media), as their selection can significantly influence the COP. The IHX cycle shows good performance for all three sinks (water, steam, air), especially when combined with R1234ze(Z) and R1233zd(E). Large temperature glides on the sink side reduce the efficiency of the system and favour the use of trans-critical cycles. Preheating the sink fluid, on the other hand, significantly increases the COP of the HP and should always be considered alongside other optimization steps during the system design. For steam generation, a combination of closed-loop HP and MVR is recommended. The results demonstrate that even at a moderate source temperature of 85 °C, efficient process heat supply is achievable, with COPs ranging from 1.11–1.97 (air), 1.94–2.75 (water) and 2.49–3.68 (steam). These values are based on conservative assumptions and can be considered as a lower bound. Reference data from HP suppliers indicate that even higher COPs are achievable. This study focuses solely on technical potential and should be complemented with economic considerations. In addition to the investment costs for the various HP cycles, costs of drilling and extracting the geothermal fluid should also be considered to improve the understanding of geothermal energy as a heat source.

Nomenclature

COP	Coefficient of performance	-
p	Pressure	Bar
P	Power	W
$\dot{Q}$	Heat flow rate	W
T	Temperature	K
$\bar{T}$	Mean temperature	K
x	Share	-

Greek symbols

η	Efficiency	-
Δ	Difference	-

Subscripts and superscripts

el	Electrical
HP	Heat Pump
L	Lorenz
th	Thermal

References

[1] BMWK, "Zahlen und Fakten: Energiedaten: Nationale und internationale Entwicklungen," 2022. Accessed: Jan. 11, 2023. [Online]. Available: https://www.bmwi.de/Redaktion/DE/Artikel/Energie/energiedaten-gesamtausgabe.html

[2] BMWK, "Zeitreihen zur Entwicklung der erneuerbaren Energien in Deutschland: unter Verwendung von Daten der Arbeitsgruppe Erneuerbare Energien-Statistik (AGEE-Stat)," 2022. Accessed: Jan. 23, 2023. [Online]. Available: https://www.erneuerbare-energien.de/EE/Navigation/DE/Service/Erneuerbare_Energien_in_Zahlen/Zeitreihen/zeitreihen.html

[3] J. W. Lund and A. N. Toth, "Direct utilization of geothermal energy 2020 worldwide review," *Geothermics*, p. 101915, 2020, doi: 10.1016/j.geothermics.2020.101915.

[4] G. HUTTRER, Ed., *Geothermal Power Generation in the World 2015-2020 Update Report*, 2020.

[5] J. W. Lund and A. N. Toth, "Direct utilization of geothermal energy 2020 worldwide review," *Geothermics*, vol. 90, p. 101915, 2021, doi: 10.1016/j.geothermics.2020.101915.

[6] S. Lassacher, S. Moser, and J. Lindorfer, "Dokumentation: Industrielle Nutzung von Geothermie," 2018. Accessed: Jan. 11, 2023. [Online]. Available: https://energieinstitut-linz.at/wp-content/uploads/2019/04/Industrielle-Nutzung-von-Geothermie_Endbericht_EIJKU_2018.pdf

[7] IEA HPT Annex 58, *High-Temperature Heat Pumps: Task 1 - Technologies* (Task Report) (Report No. HPT-AN58-2). Sweden: Heat Pump Centre, 2023.

[8] J. W. Lund, "Direct Utilization of Geothermal Energy," *Energies*, vol. 3, no. 8, pp. 1443–1471, 2010, doi: 10.3390/en3081443.

[9] T. Brasser *et al., Eds. GeoSys: Systemanalyse der geothermalen Energieerzeugung ; Teil A Synthesebericht, Teil B Ausführliche Ergebnisdokumentation* (GRS 316). Köln: GRS, 2014.

[10] gec-co, "Wissenschaftlicher Endbericht: Vorbereitung und Begleitung bei der Erstellung eines Erfahrungsberichts gemäß § 97 Erneuerbare-Energien-Gesetz: Teilvorhaben II b): Geothermie," 2019. Accessed: Jan. 12, 2023. [Online]. Available: https://www.erneuerbare-energien.de/EE/Redaktion/DE/Downloads/bmwi_de/gec-co-vorbereitung-begleitung-eeg.pdf?__blob=publicationFile&v=7

[11] M. Kaltschmitt, *Erneuerbare Energien: Systemtechnik, Wirtschaftlichkeit, Umweltaspekte,* 5th ed. Berlin: Springer Vieweg, 2013.

[12] S. Welter, "Technisch-ökonomische Analyse der Energiegewinnung aus Tiefengeothermie in Deutschland," Dissertation, Fakultät Energie-, Verfahrens- und Biotechnik, Universität Stuttgart, 2018.

[13] Graeme BEARDSMORE, Rachel WEBSTER, Behzad RISMANCHI, Kristian GJOKA, Daryl BROOKE, Ashley HALL, Martin PUJOL, Barnaby BRUCE, Simon ST HILL, Ed., *Techno-Economics of Direct Use Geothermal Energy in Gippsland, Australia*. Stanford, California, 2025.

[14] Landes Energie Argentur Hessen GmbH. "Infoportal für Großwärmepumpen: Stadtwerke Schwerin." Accessed: Apr. 7, 2026. [Online]. Available: https://grosswaermepumpen-info.de/de/projekte/details/18/

[15] A. Braun, "Mitteltiefe Geothermie und Wärmepumpen: Aktueller Stand des Aarhus Projekts,"

[16] Landes Energie Argentur Hessen GmbH. "Infoportal für Großwärmepumpen: Stadtwerke Neuruppin." Accessed: Apr. 7, 2026. [Online]. Available: https://grosswaermepumpen-info.de/de/projekte/details/58/

[17] Landes Energie Argentur Hessen GmbH. "Infoportal für Großwärmepumpen." Accessed: Apr. 7, 2026. [Online]. Available: https://grosswaermepumpen-info.de/de/projekte/?source_category=GD

[18] Allan Mahler, Birte Røgen, Claus Ditlefsen, Lars Henrik Nielsen, and Thomas Vangkilde-Pedersen, "Geothermal Energy Use, Country Update for Denmark," *European Geothermal Congress 2013*, 03 Jun., 2013.

[19] S. Klute, *Identifizierung und Bewertung von Verfahrensrouten für die industrielle Prozessdampferzeugung aus Tiefengeothermie: Am Beispiel der Papierindustrie* (UMSICHT-Schriftenreihe 106). Laufen, 2024.

[20] S. Klute and van Bek Mathias, Budr, Marcus, Eds., *Industrial process steam generation from deep geothermal reservoirs*, 2024.

[21] S. Spoelstra, "Sustainable Steam production in indutry (STEPs): Openbare eindrapportage," Petten, Niederlande, 2019. Accessed: Jan. 12, 2023. [Online]. Available: https://projecten.topsectorenergie.nl/projecten/sustainable-steam-production-for-industry-steps-24365

[22] E. Brownlie and M. Cremi, "Cornish Geothermal Distillery: BEIS Green Distilleries Competition - Phase 1," CGDC-BHE-ZZ-XX-RP-001, Mar. 2021. [Online]. Available: https://www.celsiusproject.com/

[23] B. Zühlsdorf, M. P. Andersen, and C. Tammone, "Industrial High-Temperature Heat Pumps: Task 1 – Technologies. Yearly Report 2025," doi: 10.23697/9b7b-sz34. Accessed: Apr. 7, 2026. [Online]. Available: https://heatpumpingtechnologies.org/project68/task1/

[24] A. F. Ulgado and M. T. M. Gular, Eds., *Status of Direct Use of Geothermal Energy in the Philippines*, 2005.
[25] M. Mburu, Ed., *Direct use of geothermal energy in Kenya*, 2022.
[26] T. Surana, "Development of Geothermal Energy Direct Use in Indonesia," *GHC Bulletin*, pp. 11–15, 2010.
[27] N. Chaiyat, C. Chaichana, and F. S. Singharajwarapan, "Geothermal Energy Potentials and Technologies in Thailand," *J Fundam Renewable Energy Appl*, vol. 04, no. 02, 2017, doi: 10.4172/2090-4541.1000138.
[28] M. Lauermann, V. Wilk, M. Bantle, S. Sannan, and A. Schneeberger, "DryFiciency Waste Heat Recovery in Industrial Drying Processes: Interim report on the heat pump technologies developed D4.5," 2021. Accessed: Jan. 12, 2023. [Online]. Available: https://dryficiency.eu/wp-content/uploads/2021/08/D4_5-Interim-Report-on-the-heat-pump-technologies-developed_1.pdf
[29] C. Arpagaus, F. Bless, M. Uhlmann, J. Schiffmann, and S. S. Bertsch, "High temperature heat pumps: Market overview, state of the art, research status, refrigerants, and application potentials," *Energy*, vol. 152, pp. 985–1010, 2018, doi: 10.1016/j.energy.2018.03.166.